

Structures and chaotic fluctuations of granular clusters in a vibrated fluid layerCharles C. Thomas¹ and J. P. Gollub^{1,2}¹*Department of Physics, Haverford College, Haverford, Pennsylvania 19041, USA*²*Department of Physics, University of Pennsylvania, Philadelphia, Pennsylvania 19104, USA*

(Received 12 June 2004; published 17 December 2004)

Particles that oscillate with respect to a background fluid experience a long-range attraction and a short-range repulsion that give rise to clustering at a preferred separation. We have studied the structure and dynamics of these clusters for both small ($2 < N < 7$) and large ($N=25$ or 48) clusters. For small clusters, the particles often form well-defined structures with chaotic fluctuations about the mean particle positions. However, for a given N , there are generally several different structures, e.g., both isosceles and equilateral triangles. The nearest neighbor spacings grow systematically with the dimensionless driving acceleration Γ . Large clusters are less rigid, and show much larger velocity fluctuations than do small clusters, for sufficiently large Γ . The fluctuation amplitude grows systematically with Γ for large clusters, but not for small ones. The instantaneous particle velocity is typically largest when a particle moves through a region where its probability density is low. Some of the observed phenomena suggest a variational model in which particles seek minima in an effective potential, and are perturbed by dynamically generated noise arising from the nonlinear interactions between particles. However, pairwise forces cannot account for all of the results. We discuss the nature of the fluctuations, including the low apparent dimension of the occupied set in configuration space for clusters of modest size.

DOI: 10.1103/PhysRevE.70.061305

PACS number(s): 45.70.-n, 47.55.Kf, 05.45.-a, 05.40.-a

I. INTRODUCTION

Particles that oscillate with respect to a background fluid have been shown to experience an attractive interaction that can be described as a consequence of Rayleigh streaming, a nonlinear effect that creates a secondary dipolelike flow around each particle [1]. This phenomenon can create heaping of granular materials submersed in a fluid [2], and may be of significance in connection with sedimentation or fluidized beds [3] or the clustering of spheres falling in a viscous fluid [4]. A related clustering phenomenon was seen previously in electric-field-driven suspensions of polyballs [5] that are much smaller than the granular particles studied here.

In addition to this attractive interaction, previous experiments [6] also noted a short-range repulsion between particles, again mediated by the fluid. The combination of the short- and long-range interactions creates a preferred spacing that results in the formation of ordered or disordered clusters. The previous paper focused on the mechanism of attraction and provided examples of ordered and disordered patterns. We also pointed out that fluid-mediated particle interactions provide an interesting mechanism for self-assembly of ordered structures complementary to other approaches [7].

Recently, Otto and Voth [8,9] measured the three-dimensional flow field around an oscillating sphere, and around a pair of oscillating spheres, near a solid boundary. They found that the basic streaming theory for single isolated particles must be substantially modified when a particle oscillates near a boundary, or when two particles are present. Their measurements support the basic notion that the observed particle interactions are caused by steady streaming flows, which are attractive when particles are not too close together, and repulsive at smaller separations. However, understanding the range of the repulsion and the rate of attractive approach of two particles was shown to require more

than the simple single particle flow fields proposed by Voth *et al.* [6].

In the present work we substantially extend our previous investigation, by making a systematic study of both small and large clusters. While small clusters are relatively rigid, large ones allow much more extensive particle motion within the clusters. However, in both cases, the particle spacings fluctuate due to chaotic interactions mediated by the hydrodynamics. We show that there are usually several distinct patterns for each value of N , the number of particles in the cluster. This investigation provides information about the particle interactions, and demonstrates conclusively that when more than two particles are present, the forces cannot be described by a superposition of pairwise forces. We argue that this system provides an interesting dynamical system that has both discrete and continuum aspects.

II. EXPERIMENTAL METHODS

The experimental setup has been described previously [6], and we give only a brief summary here. The experiments are conducted using a closed aluminum container that is 6 cm in diameter and 1.5 cm tall, mounted on a vertical shaft and precision bearing assembly whose purpose is to constrain the motion of the container to be vertical. The bearing is fixed on a rigid aluminum structure, and the shaft is driven from below by an electromagnetic vibrator. The vibrator is coupled to the shaft by a thin nylon threaded rod to ensure that any slight transverse misalignment of the vibrator does not affect the motion. The container is completely filled with a water-glycerol mixture of kinematic viscosity $\nu=8 \times 10^{-6} \text{ m}^2 \text{ s}^{-1}$, and an adjustable number of spherical stainless steel beads of radius $a=0.397 \text{ mm}$ and density 8.0 g/cm^3 . The bottom of the cell is a slightly concave lens of curvature radius 0.5 m ,

which is used to prevent particles from drifting to the edge of the cell due to a slight imperfection in the leveling of the cell. A small amount of NaCl is included in the fluid to make it slightly conductive, thus allowing us to ground the container to avoid charging effects.

The nondimensional acceleration is given by $\Gamma = \omega^2 S/g$, where S is the driving amplitude and g is the gravitational acceleration. Corrected for buoyancy, the acceleration would be smaller by a factor of 0.86. We use a calibrated accelerometer to determine it. The vibration causes the particles to oscillate over a depth of several particle diameters near the bottom of the fluid layer. The particle Reynolds number (based on its rms velocity, the fluid viscosity, and the particle size) is typically in the range 2–10. The particles quickly form clusters under the influence of hydrodynamically mediated forces, and we image the clusters using a fast charge-coupled device camera.

We track the particle positions using particle tracking programs written in IDL by J. C. Crocker and E. Weeks. We first find the position of each particle in each image to an accuracy of about 0.1 pixels. After determining the trajectories, we eliminate the drift of the center of mass of the cluster by redefining the positions as $\mathbf{r}'(t,p) = \mathbf{r}(t,p) - \langle \mathbf{r}(t,p) \rangle_p$, where $\mathbf{r}(t,p)$ is the position vector (x,y) at time t of particle p . The origin of these new coordinates is at the center of mass.

To calculate the mean spacings of various neighboring particle pairs, we plot a histogram $P(s)$ of pair spacings s in a given run (or time series). Most histograms use a bin size of 0.01 mm, but a few have larger or smaller ones. We usually find that a sum of Gaussian functions provides a reasonable fit to the data:

$$P(s) = \sum_{k=1}^n A_k \exp\left[-\frac{(s - s_{ck})^2}{2\sigma_k^2}\right], \quad (1)$$

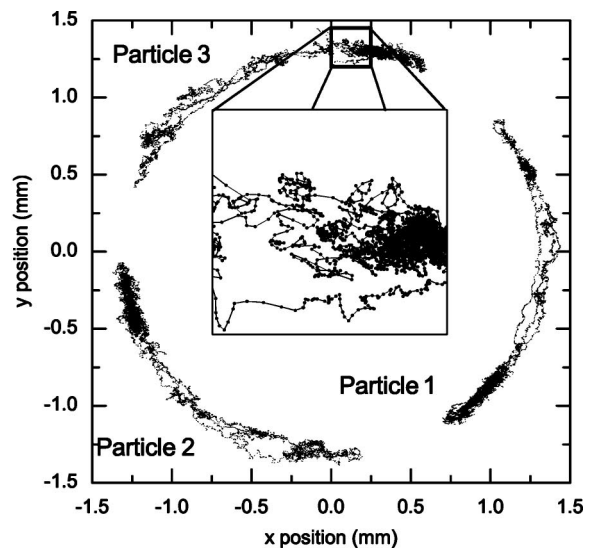
where n is the number of peaks in the distribution. From this equation, we find the parameters s_{ck} and σ_k , which are the mean neighbor spacings and the rms variations measuring fluctuations of these spacings, respectively.

The cluster structure is characterized by computing the particle number density (number per unit area as a function of the radial coordinate). It is computed in radial rings of width equal to 1 pixel.

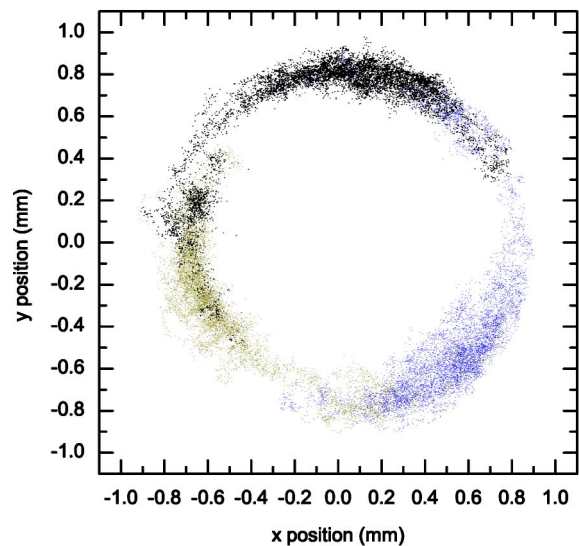
To establish the chaotic nature of the fluctuations, we compute the correlation dimension of the attractors in phase space. For a cluster of size N this computation utilizes the $2N$ time series of the coordinates. In contrast to most computations in the literature, there is therefore no need to use time delayed coordinates to reconstruct the attractor.

After determining the trajectories, we fit second order polynomials to the coordinates $x(t)$ and $y(t)$ to find the velocities. These fits use weightings $(\frac{5}{9}, \frac{8}{9}, 1, \frac{8}{9}, \frac{5}{9})$ over five adjacent points. The velocity components are then taken to be the coefficients of the quadratic terms in the fitted polynomials.

To compute the probability distribution of velocities, we use a bin size equal to $\sqrt{\langle (v_i - \bar{v}_i)^2 \rangle} / \log_{10} N$, rounded to the nearest first, second, or fifth power of ten, where N is the number of points, and v_i is the velocity component in the x



(a)



(b)

FIG. 1. (Color online) Particle trajectories vs time for $N=3$ particles, for (a) an equilateral triangle mean state (dimensionless acceleration $\Gamma=4.52$); (b) an isosceles triangle mean state ($\Gamma=2.96$). The frequency is 15 Hz here and for all subsequent figures.

or y direction. A Gaussian function is fitted to the distribution for each component, and the root mean square speed is then defined as $\sqrt{\langle v_x^2 \rangle + \langle v_y^2 \rangle}$.

III. EXPERIMENTAL RESULTS

A. Small clusters: Multiple attractors

We studied both small clusters of 2–6 particles and large ones containing 25 and 48 particles. We begin by describing the dynamics of small clusters, and then proceed to discuss large clusters.

1. $N=3$

For small clusters, there is generally more than one time-averaged configuration for a given number of particles. For

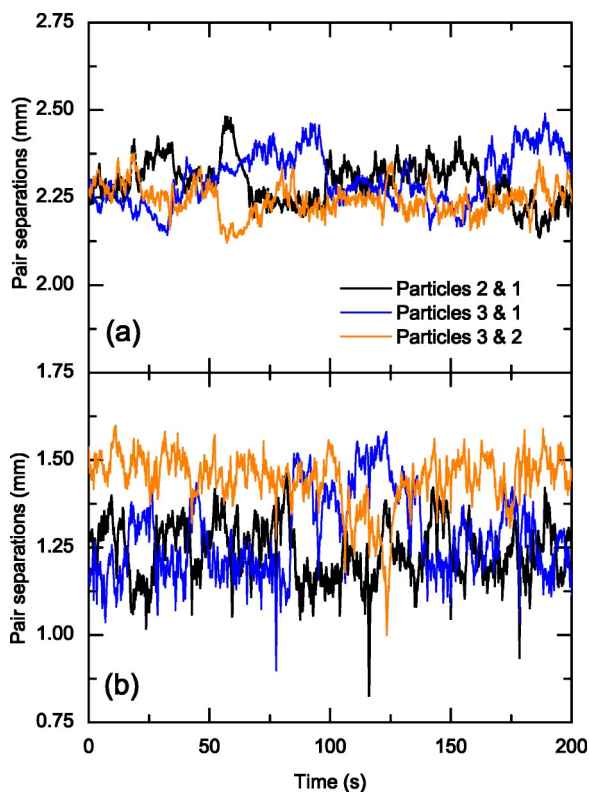


FIG. 2. (Color online) Pair separations vs time for $N=3$: (a) equilateral triangle and (b) isosceles triangle states. (Γ as in Fig. 1.) These states correspond to different attractors.

example, for three particles, we find (a) equilateral triangles, in which the spacings fluctuate, but there is a single peak in the distribution of spacings, and (b) isosceles triangles, in which there are two peaks in the distribution of particle spacings.

These features may be seen in plots of the particle trajectories as a function of time (Fig. 1), plots of pair separations vs time (Fig. 2), and plots of the distribution of pair spacings (Fig. 3) for the equilateral and isosceles cases. In Fig. 1(a) (equilateral case), it can be seen that the particles move predominantly on a ring. In Fig. 1(b) (isosceles case) we use color online to distinguish between the three particles. In this case, the ring is somewhat broader. In both cases positions fluctuate, but with greater amplitude in the azimuthal direction than in the radial direction. Some of the azimuthal variation is due to rotation of the cluster about its center of mass. In Fig. 2, the pair separations are shown to be time dependent; these variations are substantially larger than the measurement uncertainty of 0.01 mm. For the equilateral case, there is only a single peak in the distribution of particle spacings [Fig. 3(a)], while for the isosceles case, obtained for somewhat different excitation amplitude, there are two peaks. In a statistical sense, the two states are therefore quite different. These spacing distributions can be fitted reasonably well by sums of Gaussians.

The different structures found for given N seem to be attractors that can occur for different initial conditions but for the same parameters. Such a multiplicity of states is also found in other nonequilibrium systems. In all cases, the co-

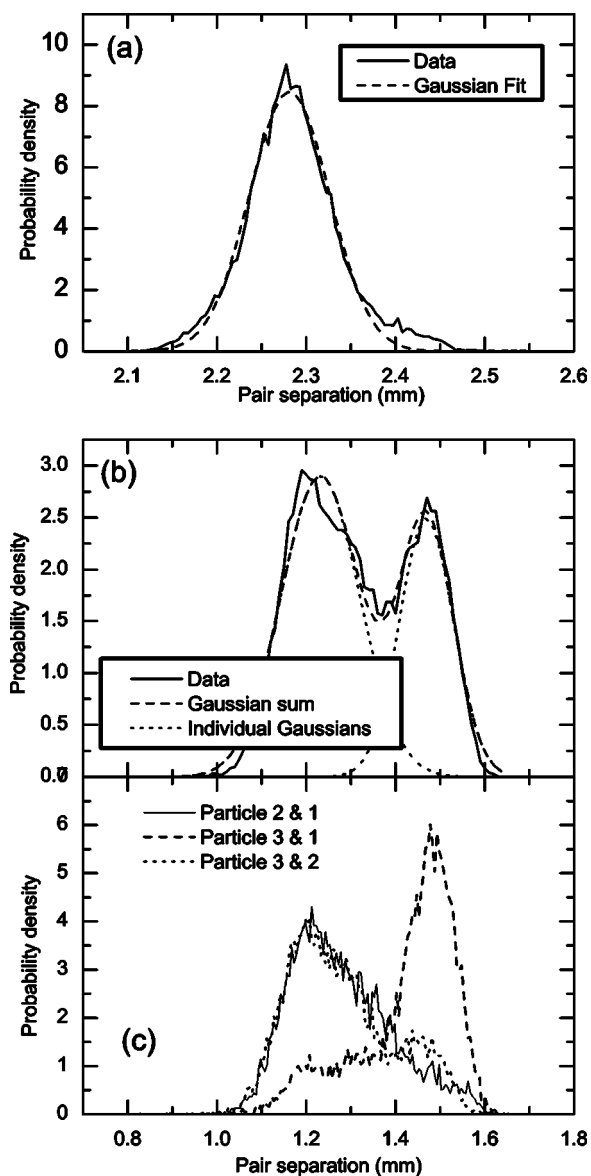


FIG. 3. Particle spacing distributions for $N=3$: (a) equilateral and (b) isosceles cases. (Γ as in Fig. 1.) In the second case, there are multiple favored spacings.

ordinates and spacings fluctuate with time. We discuss the possible causes of these fluctuations later in the paper.

2. $N=4$

The case $N=4$ adds additional complexity. In this case, the dynamical states include structures that are squares or trapezoids in the mean. The trapezoidal structure is shown in Figs. 4(a) and 4(b). Note that at $t \sim 250$ s a transition occurs. As one particle (A) moves closer to its second nearest neighbor (B), B 's nearest neighbor (C) moves away. The reverse of this transition occurs later at $t \sim 900$ s (not shown). We think of this as a noise-induced transition between different basins of attraction. Not all runs show such transitions.

3. $N=5$

The case $N=5$ includes several distinct structures: one particle surrounded by four others, equilateral pentagons, and

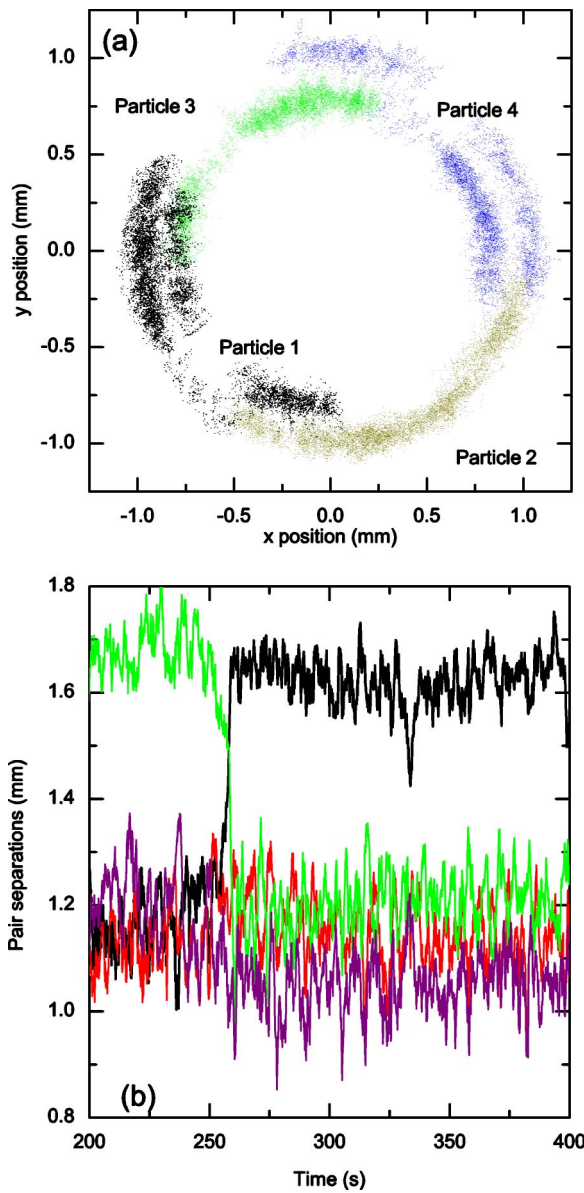


FIG. 4. (Color online) Trapezoidal case ($N=4$, $\Gamma=2.97$): (a) trajectories (b) spacings vs time. An exchange of neighbors occurs at $t=250$ s.

nonequilateral pentagons. The first of these is shown in Fig. 5 (color online). The interesting feature here is that this configuration is unstable, with nonperiodic oscillations in the pair spacings. In each transition, two distant neighbors of a central particle (3) move in, while two other neighbors recede. Then the new distant neighbors approach (3), and the new close neighbors recede. Particle 3 prefers the nearer of two alternative positions for 4 and 2, or the nearer of two alternative positions for 5 and 1, alternately in time. The exchange process recurs every 20–150 s. To follow this in the figure, the online color version is superior.

4. $N=6$ (not shown)

Here the possible structures include five particles surrounding a central one. The spacings of the members of the

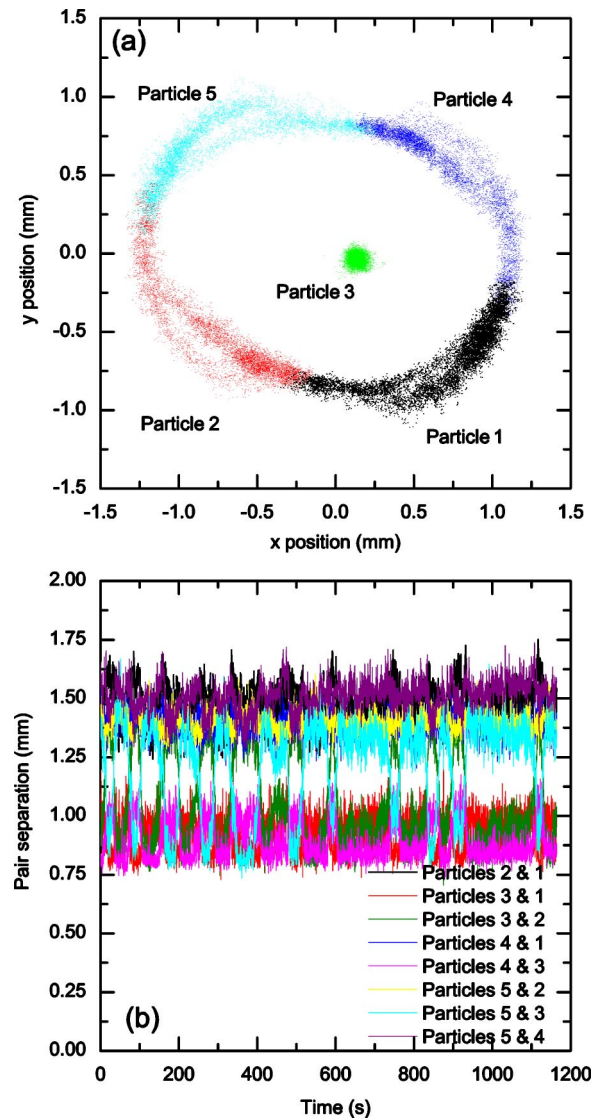


FIG. 5. (Color online) (a) Particle trajectories for $N=5$ ($\Gamma=2.96$); (b) separations vs time. Note the nonperiodic oscillation indicating repeated exchanges of neighbors (see text).

outer group are not equal. Relatively rigid equilateral hexagons also occur. The $N=6$ case illustrates a general feature of the small clusters: some are relatively rigid, while others are more flexible, in the sense that the amplitudes of the pair spacing fluctuations are larger.

B. Small clusters: Chaotic fluctuations?

Are the fluctuations of coordinates and spacings a manifestation of low-dimensional chaos? In principle there could be a large number of degrees of freedom for only a few particles, as the fluid is a continuum. We constructed the trajectories of the system in a configuration space spanned by the $2N$ coordinates, and then computed the correlation dimension to determine whether the fluctuations are low dimensional. As may be seen in Fig. 6(a) for the case $N=7$, the slope of the correlation sum (the number of points in the set within a distance R of a given point) is always quite low,

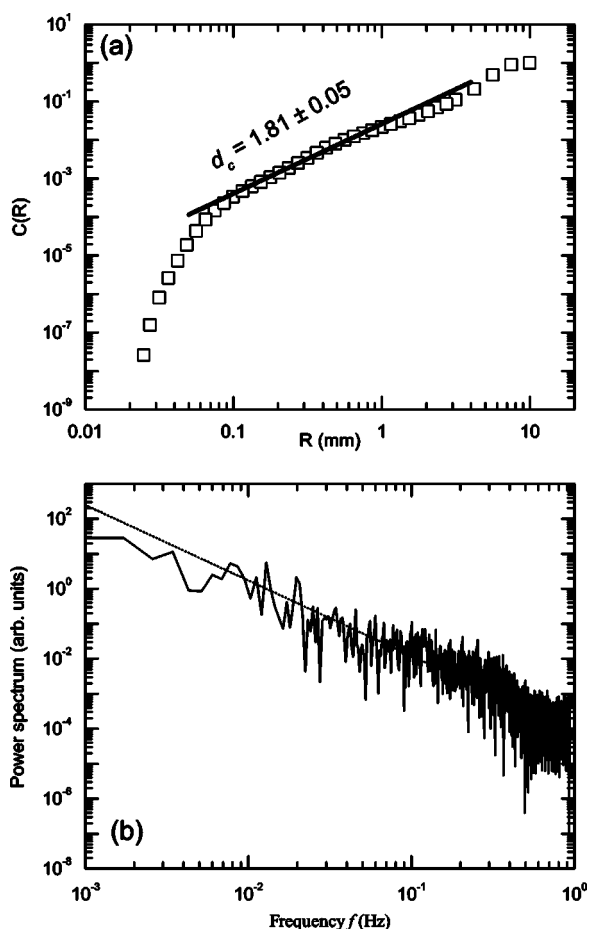


FIG. 6. (a) Calculation of the correlation dimension for $N=7$. The power law variation and low slope (about 2) indicates that the fluctuations may be regarded as chaotic for separations larger than 0.1 mm. This calculation uses all 14 time series for the x, y coordinates of the seven particles, so there is no need to use time delays to reconstruct the trajectories in phase space. (b) Power spectrum of the x coordinate of particle 1 ($N=7$, $\Gamma=2.96$). The solid line is a fit to a power law with exponent -2.2 . Similar spectra are found for particle separation time series.

about 1.8 in a configuration space of dimension 14, for separations larger than the measurement noise level, but smaller than the size of the cluster. While the precise value varies with the structure, the dimension is generally below 3 for small clusters ($N < 8$). We have not used the particle velocities in addition to their positions, because the measurement precision is less for velocities, as they have to be obtained by differentiation. Although including velocities as well as positions would presumably enlarge the correlation dimension, the present result tells us that a given particle cannot be found as a neighbor of most of the others. Rather, each particle has only a few specific neighbors, in contrast to what would occur in a sufficiently stochastic system where eventually any particle would be a neighbor of any other one.

On the other hand, the fluctuations for *very small* separations R in configuration space (< 0.1 mm) could have a stochastic component. The varying slope of the correlation sum is larger for small R , and this larger slope could be related either to stochastic influences (e.g., surface roughness of par-

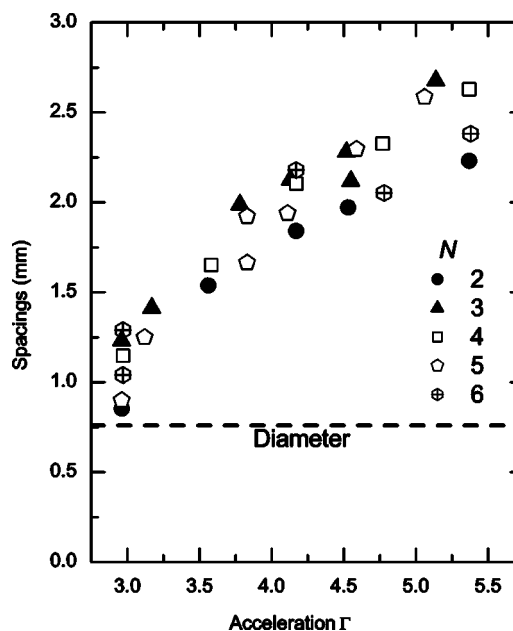


FIG. 7. Mean spacings of nearest neighbors as a function of dimensionless acceleration Γ and number of particles N . The minimum spacing is one particle diameter, shown by the dashed line.

ticles influencing their dynamics when they contact the bottom of the cell), or to measurement noise. Thus, one cannot completely exclude stochastic effects, but one can say that the variation of the correlation sum at larger spacings ($0.1 < R < 10$ mm) is consistent with low-dimensional dynamics.

We also determined power spectra of these fluctuations [Fig. 6(b)]. The spectrum is broadband and is generally well fitted by a power law with exponent close to -2 . This value is similar to the value one would find for harmonically bound particles driven by Gaussian noise. However, in the present case, the noise appears to be dynamical in origin.

C. Small clusters: General observations

The mean spacings of nearest neighbors are shown for a large number of structures for various values of the nondimensional acceleration Γ in Fig. 7. Different symbols are used for different values of the particle number N . Note the strong tendency for the mean spacing to increase with Γ . However, the mean spacing depends significantly on the specific structure, and not just on Γ . There is no strong tendency for the closest spacing to uniformly increase or decrease with increasing N .

The mean spacings are shown in Fig. 8 with bars to show the rms spacing variation (or fluctuation) for neighbors, which is a measure of the flexibility of the structure. Note that these vary over a wide range. The smallest spacing variation occurs for the two-particle case. The equilateral triangle also has a fairly small fluctuation. This makes sense because there should be no frustration with only three particles. On the other hand, for larger N , the preferred spacing (if there is one) cannot occur simultaneously for all particles. Beyond these simple cases, we are unable to predict which

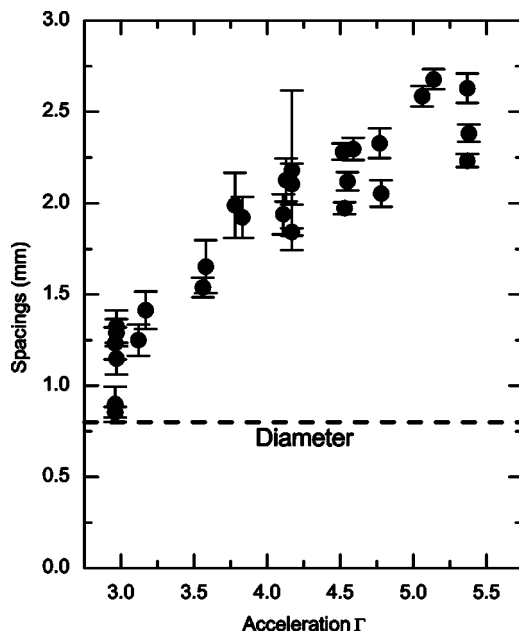


FIG. 8. Mean spacings of neighbors for $2 \leq N \leq 6$. Here, the bars indicate the rms spacing variations, a measure of the flexibility of the structure, but the number of particles in each cluster is suppressed for clarity.

structures are more flexible and hence have a larger rms spacing fluctuation.

Dynamics. For small clusters, the horizontal rms particle speed is not strongly dependent on Γ . This behavior is shown in Fig. 9. The probability distribution of any velocity component is generally non-Gaussian with extended tails.

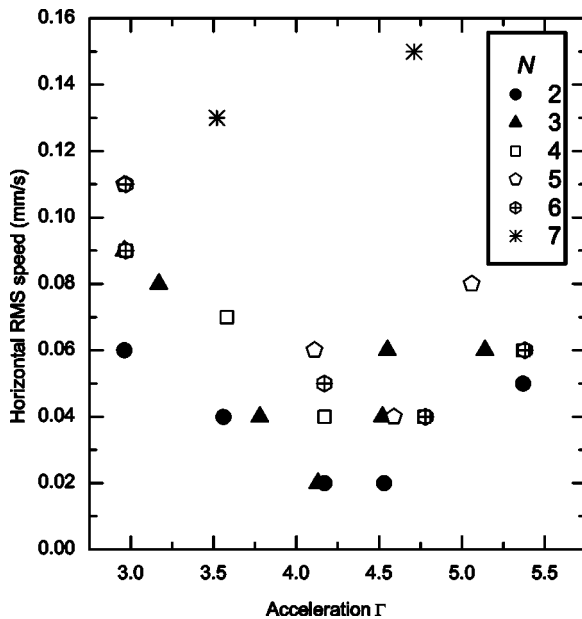


FIG. 9. Root mean square particle speed vs Γ for small clusters ($2 \leq N \leq 7$). There is no systematic dependence on Γ for small clusters.

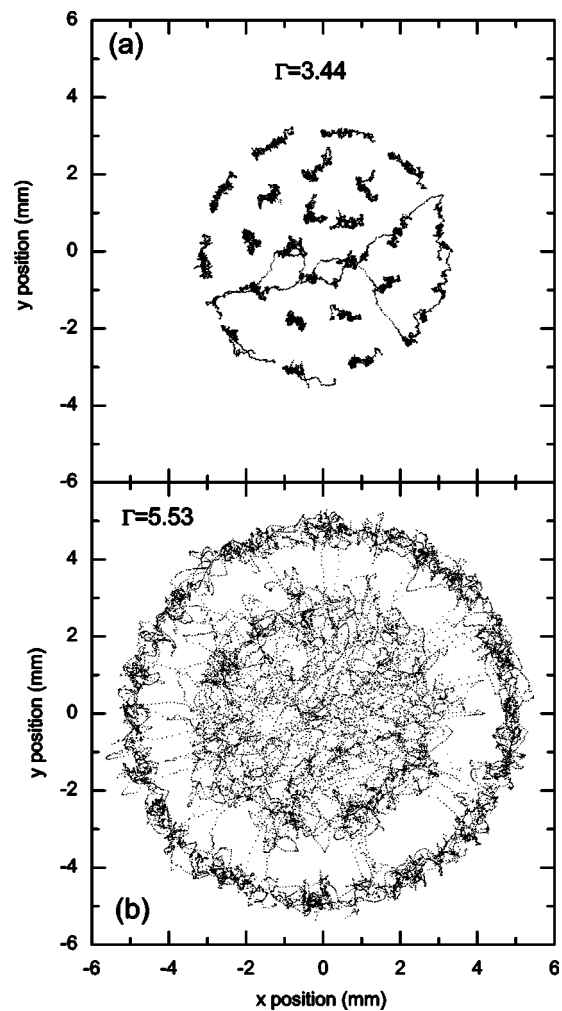


FIG. 10. Particle trajectories for a large cluster ($N=25$), for several values of Γ . In (a), at $\Gamma=3.44$, the particles fluctuate mostly about fixed positions with occasional interchanges, while in (b) ($\Gamma=5.53$) particles diffuse freely within the central core and along the outer ring.

D. Large clusters

The behavior of large clusters of 25 or 48 particles is quite different from that of the small clusters. In general, the large ones are more flexible: particles are bound less strongly to preferred positions. Typical examples are shown in Fig. 10, for $N=25$ and several values of Γ . Figure 10(a) ($\Gamma=3.44$) shows a case where the particles fluctuate predominantly around fixed positions, with occasional transitions. Figure 10(b) shows a more active case at $\Gamma=5.53$ where the particles diffuse freely in the central part of the cluster. However, those on the outer ring diffuse mainly on this ring.

In Fig. 11, we show the horizontal rms speed as a function of nondimensional acceleration. For $\Gamma < 3$, the majority of the particles are essentially in contact with each other (except for some at the periphery). For larger Γ , the particles move progressively faster as Γ is increased. This general behavior occurs for both the $N=25$ and $N=48$ clusters. Recall that a strong trend of this type was *not* observed for small clusters. This separation is due to the growth of the short-range

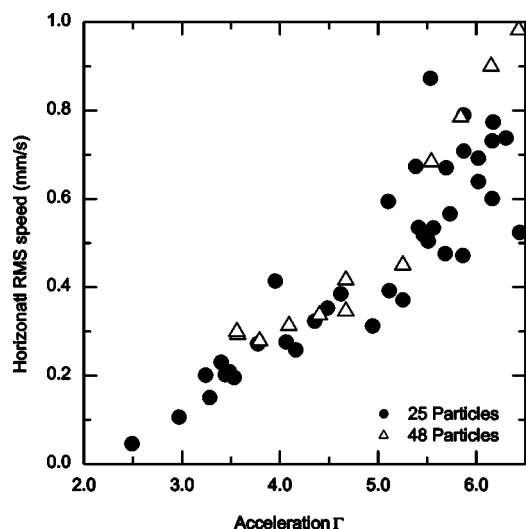


FIG. 11. Horizontal root mean square particle speed for large clusters. Most particles are in contact for $\Gamma < 3$.

repulsion of particle pairs for increasing nondimensional acceleration.

The multiplicity of states noted for small clusters also occurs for large ones. Thus, at a given value of Γ , one finds structures with horizontal rms speeds differing by a factor of 2; hence the large scatter in the data in Fig. 11.

The radial distribution function is shown in Fig. 12. There is a clearly defined outer ring, and several inner rings that overlap. We use the peak of the outer ring to define a mean cluster radius. Its variation with Γ is shown in Fig. 13. The cluster may be seen to grow monotonically with Γ as the short-range repulsion grows.

The instantaneous particle velocity is strongly anticorrelated with the local particle density, as we show in Fig. 14. The velocity is typically largest when the particle is moving through a region where the particle probability density is

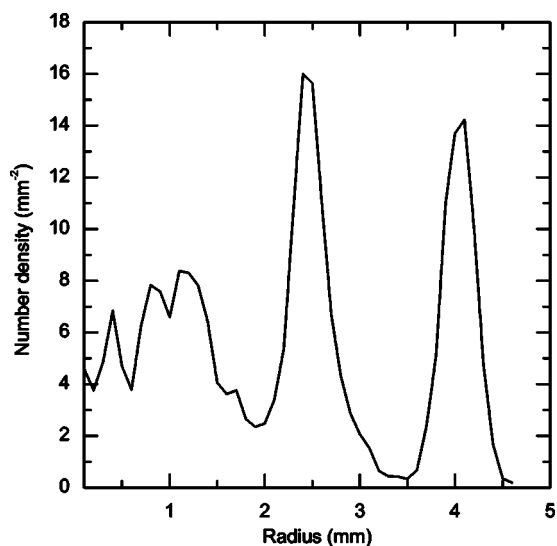


FIG. 12. Particle number density as a function of radius for $N=25$ ($\Gamma=5.53$), showing a clearly defined outer ring and an internal core with some structure.

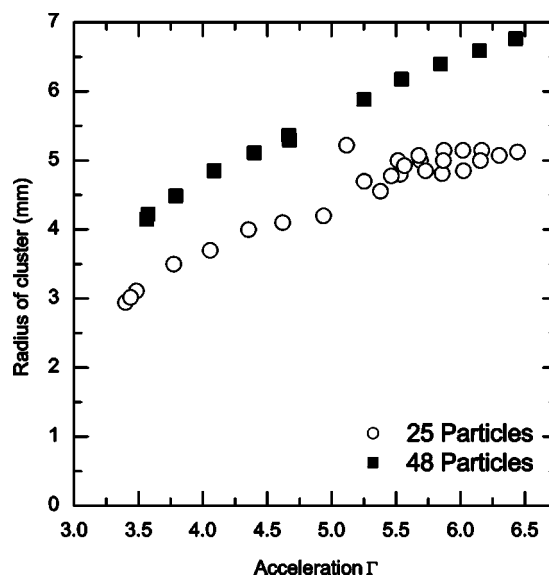


FIG. 13. Cluster radius, as indicated by the peak in the number density corresponding to the outer ring, as a function of nondimensional acceleration Γ for $N=25$ and 48. The data imply a gradual growth of the preferred pair separation with Γ in large clusters.

low, e.g., between the central core and the outer ring. This makes qualitative sense if one imagines a variational model in which the particles are driven by noise in an effective potential. However, the persistent fluctuations imply that a variational model can account for only the mean behavior, at best.

Although the particles appear to diffuse freely in the core of the cluster as shown in Fig. 15, the probability distribution of a component of the velocity is non-Gaussian; there are pronounced tails of large (or small) velocity. This behavior is shown in Fig. 16(a). In Figs. 16(b) and 16(c) we look separately at the central core of the cluster and the outer ring surrounding it. The spread of velocities, and the mean speed, are larger in the core than in the outer ring, but both are non-Gaussian. This implies that the fast jumps of particles between the core and the ring are not the only cause of the non-Gaussian tails.

Animations of the time-dependent states described in this paper are available [10].

IV. DISCUSSION AND CONCLUSION

These experimental results on the dynamics of particles with fluid-mediated interactions pose stimulating issues for theoretical consideration, and provide insights into the fluid-mediated interparticle forces.

First, our results imply that a pairwise interaction is not sufficient to explain all of the experimental results. This may be seen from the fact that the preferred spacing for $N=3$ is always greater than for $N=2$. In addition, purely additive pairwise forces could not account for the existence of both isosceles and equilateral structures at the same Γ .

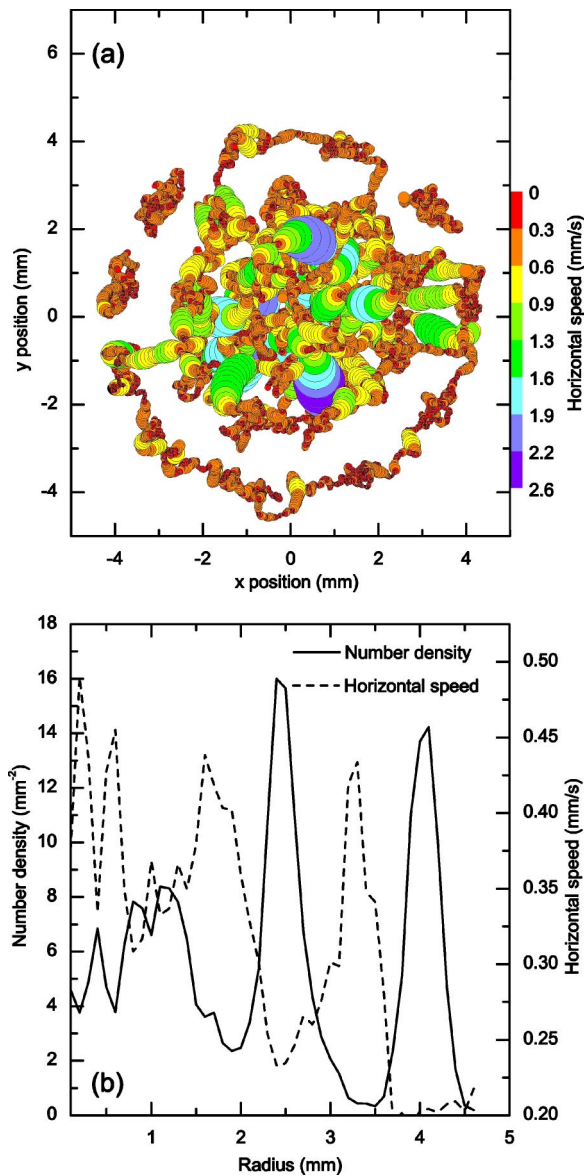


FIG. 14. (a) (Color online) Anticorrelation between instantaneous speed in the horizontal plane and particle density, for $\Gamma = 4.35$. Color and size are used to indicate velocity. Particles move quickly between the core and the outer ring. (b) The mean speed at radius r is shown along with the number density from Fig. 12, to demonstrate the anticorrelation.

What is the nature of the interaction? The previous work of Voth *et al.* demonstrated that there is both a short-range repulsion and a long-range attraction. Therefore, it is tempting to think in terms of an effective potential that is much like that of interacting neutral atoms. However, all of these states involve significant dynamical fluctuations, whereas thermal fluctuations should be exceptionally small. What is the origin of these fluctuations? One logical explanation is that they are chaotic fluctuations arising from the dynamics of the particle-fluid system. Our measurements support the hypothesis that these are indeed low-dimensional chaotic fluctuations. We know that individual isolated particles do not fluctuate significantly, and the observed collective fluctuations do not cause the particles in the small clusters to

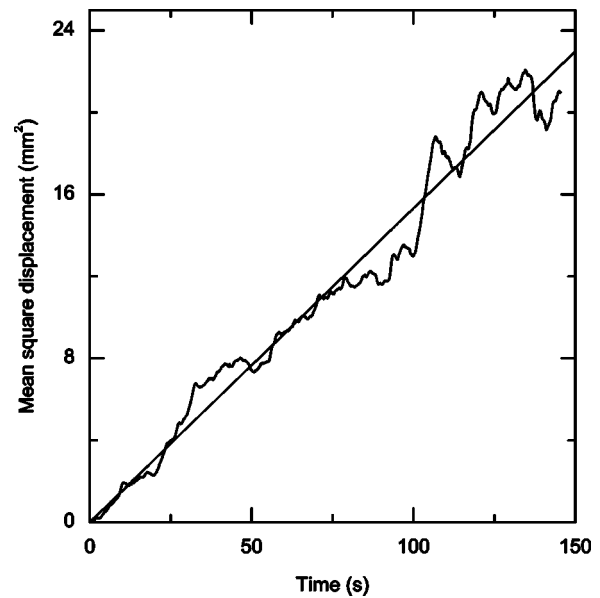


FIG. 15. Mean square particle displacement as a function of time for $N=25$, averaged over all particles. The behavior is diffusive ($\Gamma=5.25$).

explore the entire available space of allowed positions. Of course it is possible that the particles might explore more of the configuration space in a longer observation time, but the most likely hypothesis given the available evidence is that we are observing chaotic dynamics induced by the complex interaction between particles, mediated by the hydrodynamics.

The origin of the chaos is not known in detail. Do three particles moving in a fluid provide sufficient degrees of freedom at the very modest Reynolds numbers of this experiment? Each particle requires six position and velocity coordinates to describe its three-dimensional motion, so the answer would seem to be positive. On the other hand, we do see small fluctuations even for $N=2$, where the number of degrees of freedom is smaller. In this case, the smaller noise level could be due to imperfections such as the slight surface roughness of the particles, which may provide a small random element to their collisions with the driving surface. However, for $N=3$, the observed fluctuations appear to be real. It would be interesting to simulate the behavior of these clusters numerically. The chaotic dynamics may involve phase differences between the vertical oscillations of different particles.

How can we understand the expansion of the clusters as Γ is increased? Is the increase due to a growth of the preferred separation, or is it like thermal expansion in a solid, where the increasing noise at higher temperatures allows larger separations to be explored more frequently by the atoms? This question remains to be resolved.

The fluctuations of the large and small clusters behave quite differently as a function of excitation amplitude. While the small clusters do not fluctuate more rapidly as Γ is increased (Fig. 9), the opposite is true of the large clusters

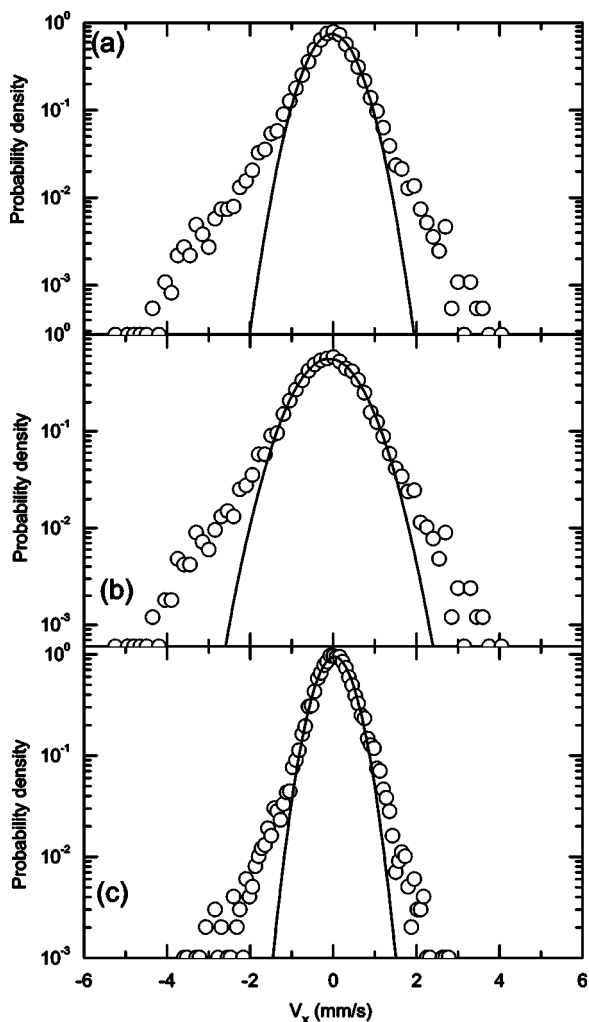


FIG. 16. (a) Probability distribution of the x component of the particle velocity in large clusters ($N=25$, $\Gamma=5.53$). Note the Gaussian core and the extended tails. In (b) and (c) we look separately at the distributions for the central core and the outer ring. The spread of velocities, and the mean speed, are larger in the core than in the outer ring.

(Fig. 11). It is tempting to think of Γ as a surrogate for temperature, and the interactions as being approximately described by an effective potential. However, the data show that thinking of Γ as an effective temperature is not a fully

adequate approach. The reason may be that although the dynamical noise grows with Γ , the forces do also, so that the particles are trapped in deeper potential wells as Γ is increased for small clusters. For large clusters, on the other hand, the balance between these two effects is finally tipped toward larger fluctuations with increasing Γ . When a particle has many neighbors, there are a large number of neighboring configurations where all the particles experience little net attraction or repulsion, and hence are easily perturbed by the ambient dynamical noise. One can perhaps think of this as many comparable local minima of an effective potential, separated by small barriers.

The notion that chaotic fluctuations arising from deterministic internal dynamics can behave similarly to stochastic (external) noise has been suggested from time to time in fluid systems [11]. Here we have a situation where this seems to be roughly the case.

We leave for future work the exploration of the role of viscosity in this problem, because a substantial investigation would be required given the diversity of phenomena documented here. The influence of the viscosity on the interparticle forces is probably not fully captured by the Reynolds number alone (based on the particle's rms velocity and size, and the fluid's viscosity). The velocity variation during the bouncing trajectory, and hence the streaming flow and interparticle force, depends also on the forcing conditions, and on the relative importance of gravity and viscosity.

An interesting problem for the future is to relate the clustering phenomena described in this paper to quantitative measurements of the mediating flow field such as those made by Otto and Voth [9]. However, the dynamic interactions between multiple particles documented here introduce additional complexity beyond that manifested in their work on fixed particle pairs. A quantitative understanding of multiparticle fluid-mediated interactions remains somewhat out of reach at present.

ACKNOWLEDGMENTS

This work was supported in part by NSF Grants No. DMR-0072203 and No. DMR-0405187 to Haverford College. We appreciate helpful conversations with Tom Lubensky, Lyle Roelofs, and Greg Voth.

-
- [1] N. Riley, *Annu. Rev. Fluid Mech.* **33**, 43 (2001).
 - [2] J. M. Schleier-Smith and H. A. Stone, *Phys. Rev. Lett.* **86**, 3016 (2001); H. K. Pak, E. Van Doorn, and R. P. Behringer, *ibid.* **74**, 4643 (1995).
 - [3] A. F. Fortes, D. D. Joseph, and T. S. Lundgren, *J. Fluid Mech.* **177**, 467 (1987).
 - [4] K. O. L. F. Jayaweera, B. J. Mason, and G. W. Slack, *J. Fluid Mech.* **20**, 121 (1964).
 - [5] P. Richetti, J. Prost, and N. A. Clark, in *Physics of Complex and Supermolecular Fluids*, edited by S. A. Safran and N. A. Clark (Wiley, New York, 1987), p. 387.
 - [6] G. A. Voth *et al.*, *Phys. Rev. Lett.* **88**, 234301 (2002).
 - [7] M. Trau, D. A. Saville, and I. A. Aksay, *Science* **272**, 706 (1996); S. R. Yeh, M. Seul, and B. I. Shraiman, *Nature (London)* **386**, 57 (1997); T. Gong and D. W. M. Marr, *Langmuir* **17**, 2301 (2001); B. A. Grzybowski, H. A. Stone, and G. M. Whitesides, *Nature (London)* **405**, 1033 (1997).
 - [8] F. Otto, Diplomarbeit, Universität Regensburg, 2004.
 - [9] F. Otto and G. Voth (private communication).
 - [10] Video animations showing the time-dependent states discussed in this paper are available at <http://www.haverford.edu/physics-astro/gollub/clustering/>
 - [11] M. C. Cross and P. C. Hohenberg, *Rev. Mod. Phys.* **65**, 851 (1993).